arXiv:1407.0747v1 [cond-mat.supr-con] 3 Jul 2014

Identification of the crystal structures of two superconducting phases for potassium-doped picene

Xun-Wang Yan[1,2,3,4], Zhongbing Huang[1,2,*] and Hai-Qing Lin[1]
[1] *Beijing Computational Science Research Center, Beijing 100084, China*
[2] *Faculty of Physics and Electronic Technology, Hubei University, Wuhan 430062, China*
[3] *State Key Laboratory of Theoretical Physics, Institute of Theoretical Physics, Chinese Academy of Science, Beijing 100190, China and*
[4] *School of physics and electrical engineering, Anyang Normal University, Henan 455000, China*
(Dated: July 4, 2014)

By the first principles calculations and X-ray diffraction simulations, we perform a systematic study of multiple superconducting phases of potassium-doped picene [Nature **464** 76, 2010]. The combination of optimized lattice parameters, formation energy, and simulated X-ray diffraction spectra indicates that the superconducting phase with transition temperature (T_c) of 7 K corresponds to a charge doped K_2picene, which is semiconducting with a 0.1 eV energy gap, while the superconducting phase with T_c=18 K corresponds to a metallic K_3picene. The distinct crystal and electronic structures of K_2picene and K_3picene provide a reasonable explanation of two superconducting phases in potassium-doped picene.

Superconductivity in organic materials are among the most fascinating phenomena in condensed matter physics. The recent discovery of superconductivity in potassium-doped picene ($C_{22}H_{11}$) [1] stimulated great interest of researchers to investigate superconductivity in aromatic solid materials. A few kinds of aromatic molecules, including picene ($C_{22}H_{11}$), phenanthrene ($C_{14}H_{10}$) [2], coronene ($C_{24}H_{12}$) and dibenzopentacene ($C_{30}H_{18}$)[3] have been used to synthesize aromatic superconductors by intercalating metal atoms into the molecular crystals [4, 5]. Experimental measurements [6–9] and theoretical calculations [10–14] showed that there exist electronic correlations, magnetism [15–19], and pronounced electron-phonon coupling [20] in aromatic superconductors, which are very similar to the situations of high-T_c cuprates and iron-based superconductors. Hence, it is challenging to understand the superconducting (SC) mechanism in aromatic superconductors.

One of the most intriguing properties of aromatic superconductors is the existence of multiple SC phases in K-doped picene, coronene, and dibenzopentacene. In particular, two different SC phases in K-doped picene, one with $T_c \sim 7$ K and the other as high as 18 K, have attracted considerable attention. Currently, the crystal structures of K-doped picene remain unclear. On the experimental side, the measured lattice parameters showed large discrepancies for the samples prepared by solid-state reaction method and solution method (see Table I), and it is difficult to derive the positions of intercalated K atoms. On the theoretical side, the optimized crystal structures from the first principles calculations deviate dramatically from the experimental ones: the experimental lattice parameter a is much larger than b, while a and b take similar values from the first principles simulations.

Since the determination of atomic structure of materials is a prerequisite to explore their electronic, magnetic, and SC properties, it is urgent to identify the crystal structures of aromatic superconductors, especially for two SC phases in K-doped picene, where various experimental data have been accumulated. Besides aromatic superconductors, the identification of crystal structure is crucial for understanding the SC property of other alkali metal intercalated layered materials, including iron-based superconductors, graphite, and graphene. Interesting, in FeSe, alkali metal (Li, Na, or K) has been intercalated into the space between FeSe layers to optimize the SC property, which also leads to multiple SC phases at T_c=30∼46K.

In this Letter, we have performed a systematic study of two SC phases in K-doped picene by combining the first principles calculations and X-ray diffraction (XRD) simulations. Based on the optimized lattice parameters, formation energy, and XRD spectra, we find that the SC phase with $T_c \sim 7$ K is indeed related to a semiconducting K_2picene, whereas the SC phase with $T_c = 18$ K corresponds to a metallic K_3picene. This is the first time to identify theoretically the difference of crystal structures and dopant concentrations between two different SC phases. The relatively large density of states of 10.4 states/eV at the Fermi level in K_3picene provide a reasonable explanation of higher T_c in the $T_c = 18$ K SC phase. In addition, we point out that an inclusion of KOH in SC samples not only explains the experimental XRD peaks, but also demonstrates that preventing KOH generation in experiment is an important measure to improve the sample quality of K-doped aromatic superconductors.

In our calculations the plane wave basis and pseudopotential method was used. The psudopotentials are supplied by Vienna Ab initio simulation package (VASP) website [21, 22], which adopt the projector augmented-wave method (PAW) [23] and Perdew-Burke-Ernzerhof (PBE) type generalized gradient approximation (GGA) [24]. The plane wave basis cutoff is set to 300 eV. The Gaussian broadening technique was used and a mesh of $4 \times 6 \times 4$ k-points were sampled for the Brillouin-zone

* huangzb@hubu.edu.cn

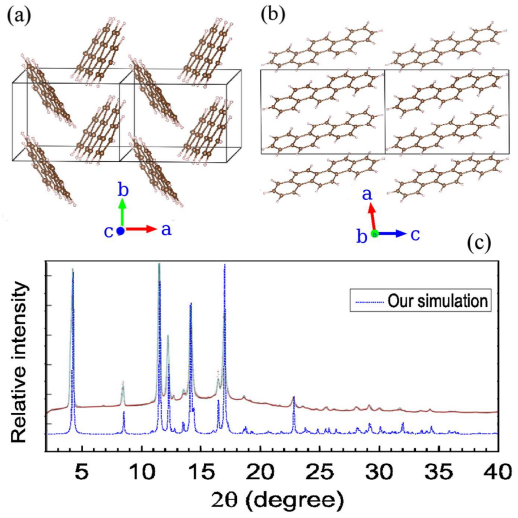

FIG. 1. (Color online) The intralayer arrangement of molecules (a) shown in a $2 \times 1 \times 1$ supercell, and the interlayer arrangement of molecules (b) shown in a $1 \times 1 \times 2$ supercell. (c) our simulated XRD spectra (blue line), and the experimental one (black circles and red line) adapted by permission from Macmillan Publishers Ltd: Nature **464** 7285 (Fig. S7), R. Mitsuhashi *et al*, copyright (2010). The used X-ray wave length is 0.99937 Å.

integration. The convergence thresholds of the total energy, force on atom and pressure on cell are 10^{-4} eV, 0.01 eV/Åand 0.1 KBar, respectively. The XRD sepectra were simulated by Mercury program [25].

We first study the structure of pristine picene, which is the basis for the structure exploration of K-doped counterpart. Picene molecule is a flat hydrocarbon composed of five fused benzene rings. The molecular crystal of pristine picene crystallizes in the space group $P2_1$ and each unit cell contains two molecules, which are arranged in a herringbone pattern to form a layer parallel to the ab plane, and then molecular layers are stacked along the c axis, as shown in Figs. 1(a) and 1(b). The optimized lattice parameters a, b, c, β are 8.489 Å, 6.124 Å, 13.444 Å, 90.43°, in excellently agreement with the experimental values 8.472 Å, 6.17Å, 13.538 Å, 90.84°). The simulated XRD spectra of picene shown in Fig. 1(c) are in perfectly consistent with the measured ones. These results provide a fundamental guarantee for the applicability of C and H pseudopotentials, the reasonability of k-point mesh, and plane wave basis cutoff in our following calculations of K-doped picene.

Experimental results indicated that K-doped picene also crystallizes in the space group $P2_1$ and two molecules in a unit cell arrange in the herringbone pattern. In order to distinguish the K atom positions in the molecular crystal, we define the interstitial space enclosed by four molecules in a molecular layer as a hole, and name the positions corresponding to five benzene rings of a molecule as A, B, C, D, E, as shown in Fig. 2(a). When two K atoms are intercalated into each hole, three kinds of possible configurations with $P2_1$ symmetry can be formed, which are called as K_2-BD, K_2-AC, and K_2-CE shown in Figs. 2(c), (d), and (e). The configurations are named after their K atom positions. Fig. 2(b) displays the positions of K atoms and molecules viewed along the c axis for K_2-BD, and the other two phases have a similar arrangement.

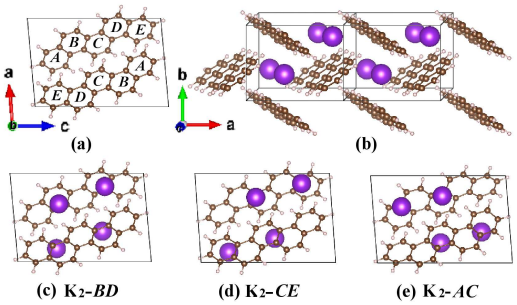

FIG. 2. (Color online) (a) Five favorable positions of K atom in the interstitial space viewed along b axis, named as A, B, C, D, E corresponding to five benzene rings repectively. (b) A schematic diagram of K atom arrangement for K-doped picene. (c), (d) and (e) are three possible structure phases for K_2picene.

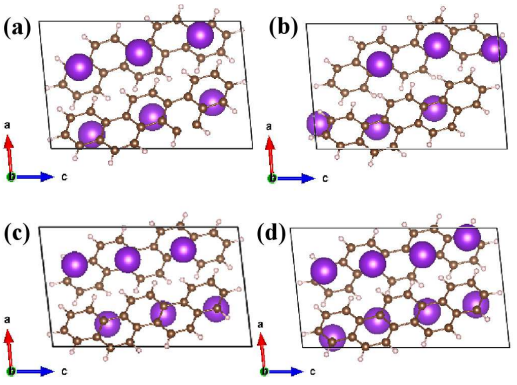

FIG. 3. (Color online) A schematic diagram of three possible structure phases for K_3picene, named as K_3-I (a), K_3-II (b), K_3-III (c), and K_4picene (d).

The structural phases of K_3picene can be constructed by adding two K atoms to the unit cell of K_2picene phase. On the basis of K_2-AC or K_2-CE, the occupation with K atom at the E or A position lead to the K_3-I phase, as shown in Fig. 3(a). When two K atoms are added to the K_2-BD cell, there are two kinds of arrangement, *i.e.*, two K atoms are put outside E and outside A, corresponding to the initial configuration of phases K_3-II and K_3-III. The structure of K_3-II is similar to K_2K_1 in Ref. [10] and two K atoms still sit outside E positions after relaxation shown in Fig. 3(b). However, K atoms outside A position in the K_3-III phase have a large change and move into the hole after structure optimization shown in Fig. 3(c).

The optimized lattice parameters and fraction coordi-

TABLE I. The optimized lattice parameters a, b, c, β, the fraction coordinations of the doped K atoms and the space group of unit cell for K_2picene and K_3picene with different structural phases.

	a (Å)	b (Å)	c (Å)	β (°)	space group
K_2-BD	8.766	6.818	13.166	95.13	$P2_1$
	(0.3461	0.2917	0.6540)		
	(0.1500	0.3017	0.2981)		
K_2-CE	8.752	6.556	13.293	92.98	$P2_1$
	(0.2571	0.3062	0.5452)		
	(0.1073	0.2856	0.1980)		
K_2-AC	8.651	6.524	13.306	92.60	$P2_1$
	(0.3150	0.3269	0.8168)		
	(0.2352	0.3291	0.5126)		
Exp. [1]	**8.707**	**5.912**	**12.97**	**92.77**	$P2_1$
K_3-I	8.675	6.770	13.669	95.53	$P2_1$
	(0.3611	0.3057	0.8222)		
	(0.2470	0.2913	0.5183)		
	(0.1098	0.2912	0.2074)		
K_3-II	8.914	6.793	13.534	94.72	$P2_1$
	(0.3227	0.2953	0.6336)		
	(0.1753	0.2949	0.3250)		
	(0.2013	0.2372	0.0257)		
K_3-III	8.523	6.838	14.058	96.67	$P2_1$
	(0.2732	0.3048	0.5729)		
	(0.1904	0.2976	0.2882)		
	(0.3153	0.2897	0.8434)		
Exp. [6]	**8.571**	**6.270**	**14.01**	**91.68**	$P2_1$

nations of K atoms are listed in Table. I. For K_2 picene, the energy of K_2-BD is lower than that of K_2-CE by 0.28 eV/molecule and that of K_2-AC by 0.41 eV/molecule, suggesting that the K_2-BD phase is the most stable configuration for K_2picene from the energetic point of view. As a result, the K_2-BD phase has a higher probability of existence in the experimental samples. Among the three phases for K_3picene, K_3-I has the lowest energy, which is 0.46 eV and 0.022eV lower than K_3-II and K_3-III per unit cell, respectively. Notice that K_2-BD and K_3-I are in good agreement with the $K_{2.9}$ sample [1] and the T_c=18 K sample [6], except for a bit longer b axis.

We also calculate the formation energy in term of the formula $E_{formation} = E_{Kx} - E_{pristine} - E_{dopant}$, where x stands for the number of K atoms and E_{dopant} is the product of single atom energy in bulk metal and atom number in a unit cell. For the K_2-BD phase, the formation energy is -0.330 eV per K atom, which suggests that it is easy to synthesize in experiment. The formation energy of the K_3-I phase is -0.295 eV per K atom, comparable to the one for K_2picene, indicating that K_3picene is another reasonable structure phase for K-doped picene. For K_4picene as shown in Fig. 3(d), the corresponding formation energy is -0.067 eV per K atom, much less than the ones for K_2picene and K_3picene, indicating that K_4picene is not a stable structural phase.

Having identifying the stable structure phases for K-doped picene, we now turn to identify the crystal structure of experimental SC samples. In Fig. 4, we compare

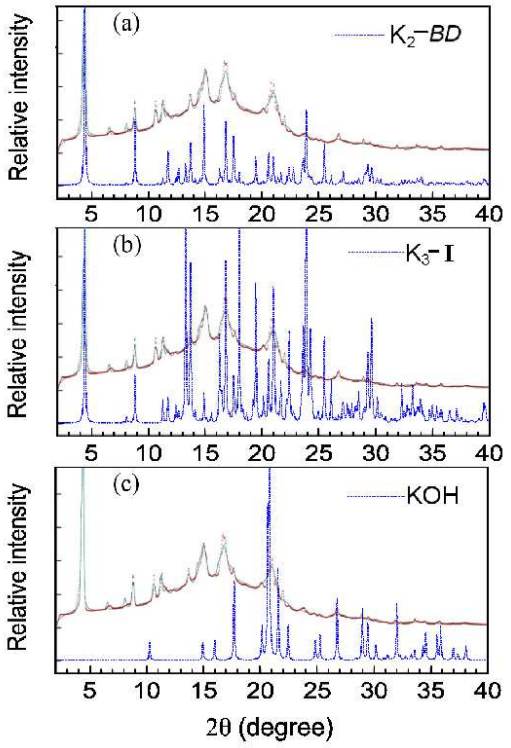

FIG. 4. (Color online) The simulated XRD spectra of K_2-BD phase (a) and K_3-I phase (b) based on the experimental lattice parameters [1]. (c) The XRD spectra of KOH with the experimental crystal structure. The experimental XRD spectra (black circles and red line) of $K_{2.9}$picene adapted by permission from Macmillan Publishers Ltd: Nature **464** 7285 (Fig. S7), R. Mitsuhashi *et al*, copyright (2010). The used X-ray wave length is 0.99937 Å.

the simulated XRD spectra of K_2-BD and K_3-I with the measured results for the sample with T_c=7K [1]. For both K_2-BD and K_3-I, we fix the lattice parameters at experimental values to relax the inner atoms. One can clearly see that the simulated XRD spectra of K_2-BD is in good agreement with the measured one, which can be seen from the positions and strength of the main XRD peaks shown in Fig. 4(a). The z fraction coordinations for two independent K atoms are (0.3127, 0.6626), which is close to ($\frac{1}{3}$, $\frac{2}{3}$), similar to the z coordinations (0.2981, 0.6540) in the full relaxation case. In contrast, the XRD structure of K_3-I is not consistent with the expeimental one. Based on the above analysis on energy and XRD spectra, we can draw a conclusion: the $T_c \sim 7$ K SC phase corresponds to K_2picene with a K_2-BD structure.

In Fig.5, the simulated XRD spectra are compared with the experimental measurement for the T_c = 18 K phase by a solution method [6]. The XRD spectra of K_3-I based on the experimental lattice parameters as displayed in Fig.5(a) show that the peak positions below 28 degree are in accordance with the experiment. Our results (not shown here) also indicate that the XRD spectra for K_3-II and K_3-III have a stronger discrepancy to the experiment

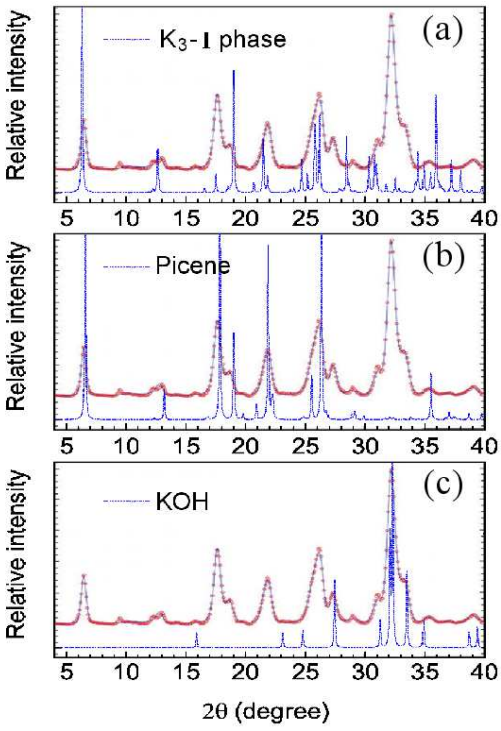

FIG. 5. (Color online) The simulated XRD spectra of K_3-I phase (a) based on the experimental lattice parameters [6] and the XRD spectra of pristine picene (b) and KOH (c) with the experimental crystal structure, ploted with bright blue line. The experimental XRD spectra (red circles and blue line) of K_3 picene is also presented in three panels, which data is from Ref. [6]. The used X-ray wave length is 1.54056 Å.

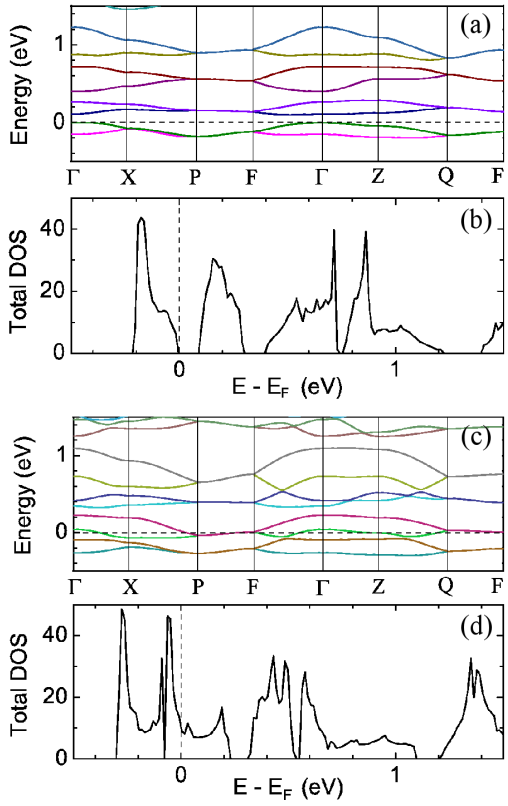

FIG. 6. Energy bands and density of states for K_2-BD phase (a) (b) and K_3-I (c) (d). Fermi energy is set to zero.

than K_3-I. For this reason, the K_3-I phase is the most possible configuration corresponding to $T_c = 18$ K phase. As seen from Figs.5(b) and (c), the XRD peaks of pristine picene and KOH have a good agreement with the experimental ones, suggesting that pristine picene and KOH have a considerable portion in the SC sample. This can explain the reason of XRD spectra difference in Fig. 5(a) and the fact of small superconductive shielding fraction.

The band structure and DOS of K_2-BD and K_3-I are presented in Fig. 6. On the whole the bands are flat and little dispersive. For K_2-BD phase, two bands below Fermi level are mainly from the lowest unoccupied molecular orbitals (LUMO) of two molecules in a unit cell in Fig. 6 (a), which are occupied as a result of the intercalation of two K atoms per molecule. For K_3-I phase of K_3picene, the Fermi level crosses the two bands coming from LUMO+1 orbitals. K_2-BD phase is a semiconductor with an energy gap of 0.1 eV, which is the parent compounds for $T_c = 7$ K SC phase in terms of above analysis. When the concentration of K atom has few percents deviation from 2 in K_2-BD phase of K_2picene, similar to electron or hole doping, the superconductivity can occur. The K_3-I phase is a metal with relatively high DOS value of 10.4 states/eV per unit cell at Fermi level. The great difference of electronic structure between K_2-BD and K_3-I can lead to different superconducting phases, and also lead to different pressure effect on the superconducting T_c [6]. According to Bardeen-Cooper-Schrieffer theory of electron-phonon induced superconductivity, the high DOS value of 10.4 states/eV suggest that K_3-I phase is related to the superconducting phase of $T_c = 18$ K.

Finally, we analyze the structural feature of K_3-I phase. The K atoms located at the A, C, E positions, which is the most uniform distribution for K_3picene. The length of a hole accommodating K atoms is about 13.76 Å, equal to the molecule length. It assure that two neighbor K atoms have an appropriate distance of 4.18∼4.30 Å, which is close to the distance of 4.54 Å in the bulk metal of potassium. This uniform distribution can also be found out by the fraction coordinations (z_1=0.2074, z_2=0.5183 z_3=0.8222) of three K atoms listed in Table. I. Another feature is that the picene molecule keep in a plane perfectly for K_3-I phase due to K atoms uniform distributions. The superconductivity is correlated intimately to the conjugated π orbitals in K-doped phenanthrene and picene, similar to K or Ca intercalated graphite. The uniform distribution of K atoms helps charge to be transferred to molecules and the planar molecule with the least distortion helps delocalize π electrons throughout the whole molecule. Therefore, the

K_3-I phase is favorable for higher SC T_c.

In conclusion, we have performed first principle calculations and XRD simulation for K-doped picene. Our results suggest that K_2picene with K_2-*BD* phase is the parent compound of T_c =7 K superconducting phase, while the K_3-I of K_3picene corresponds to the superconducting phase with T_c of 18 K. K_2-*BD* phase is semiconducting with 0.1 eV energy gap and K_3-I phase is a good metal. The great difference in electronic properties leads to different T_c and pressure effect on T_c in two superconducting phases. The existence of KOH in K-doped picene sample can explain the experimental XRD peaks. Meanwhile, the generation of KOH is an important factor to decrease the sample quality. In a word, we determine the crystal structures of two superconducting phases in K-doped picene, and provide an important basis to further theoretical and experimental studies.

Acknowledgments: We acknowledge Cai-Zhuang Wang for interesting suggestion and fruitful discussion on XRD simulation. This work was supported by MOST 2011CB922200, the Natural Science Foundation of China under Grants Nos. 91221103, 11174072 and U1204108.

[1] R. Mitsuhashi *et al*, Nature **464**, 76 (2010).
[2] X. F. Wang *et al*, Nat. Commun. **2**, 507 (2011).
[3] M. Xue *et al*, Sci. Rep. **2**, 389 (2012).
[4] X. F. Wang *et al*, Phys. Rev. B **84**, 214523 (2011).
[5] X. F. Wang *et al*, J. Phys. Condens. matter **24**, 345701 (2012).
[6] T. Kambe *et al*, Phys. Rev. B **86**, 214507 (2012).
[7] K. Teranishi *et al*, Phys. Rev. B **87**, 060505 (2013).
[8] A. Ruff *et al*, Phys. Rev. Lett. **110**, 216403 (2013).
[9] M. Caputo *et al*, J. Phys. Chem. C **116**, 19902 (2012).
[10] T. Kosugi, T. Miyake, S. Ishibashi, R. Arita, and H. Aoki, Phys. Rev. B **84**, 214506 (2011).
[11] P. L. de Andres, a. Guijarro, and J. A. Vergés, Phys. Rev. B **83**, 245113 (2011).
[12] P. L. de Andres, a. Guijarro, and J. A. Vergés, Phys. Rev. B **84**, 144501 (2011).
[13] S. S. Naghavi, M. Fabrizio, T. Qin, and E. Tosatti, Phys. Rev. B **88**, 115106 (2013).
[14] X.-W. Yan, Z. Huang, and H.-Q. Lin, J. Chem. Phys. **139**, 204709 (2013).
[15] M. Kim, B. I. Min, G. Lee, H. J. Kwon, Y. M. Rhee, and J. H. Shim, Phys. Rev. B **83**, 214510 (2011).
[16] G. Giovannetti and M. Capone, Phys. Rev. B 83, 134508 (2011).
[17] M. Kim, H. C. Choi, J. H. Shim, and B. I. Min, New J. Phys. **15**, 113030 (2013).
[18] Z. Huang, C. Zhang, and H.-Q. Lin, Sci. Rep. **2**, 922 (2012).
[19] J. A. Vergés *et al*, Phys. Rev. B **85**, 165102 (2012).
[20] T. Kato, T. Kambe, and Y. Kubozono, Phys. Rev. Lett. **107**, 077001 (2011).
[21] G. Kresse and J. Hafner, Phys. Rev. B **47**, 558 (1993).
[22] G. Kresse and J. Furthmüller, Phys. Rev. B **54**, 11169 (1996).
[23] P. E. Blöchl, Phys. Rev. B **50**, 17953 (1994).
[24] J. P. Perdew, K. Burke, and M. Ernzerhof, Phys. Rev. Lett. **77**, 3865 (1996).
[25] Mercury, Crystal Structure Visualization and Exploration Program, http://www.ccdc.cam.ac.uk/products/mercury (2014).